Hindawi Publishing Corporation
Advances in Condensed Matter Physics
Volume 2013, Article ID 250301, 10 pages
http://dx.doi.org/10.1155/2013/250301

Research Article

$ZnO_{1-x}S_x$ Nanosphere in Ferroelectric Liquid Crystal Matrix: The Effect of Aggregation and Defects on the Dielectric and Electro-Optical Properties

Dharmendra Pratap Singh, Swadesh Kumar Gupta, and Rajiv Manohar

Liquid Crystal Research Lab, Physics Department, University of Lucknow, Lucknow 226007, India

Correspondence should be addressed to Rajiv Manohar; rajiv.manohar@gmail.com

Received 31 May 2013; Revised 20 July 2013; Accepted 20 July 2013

Academic Editor: David Huber

High concentration (5 wt %) of $ZnO_{1-x}S_x$ nanosphere (NS) has been dispersed in the ferroelectric liquid crystal (FLC) to analyze the effect of high dopant concentration in the FLC matrix. The FLC molecules actively interact with the NS. The presence of NS enhances the photoluminescence of the pure FLC material due to the coupling of localized surface plasmon resonance from NS with FLC molecules. The high concentration of NS causes an aggregation in the FLC matrix and creates topological defects. The defects and aggregation cause the change in electro-optical and dielectric properties of the pure FLC material. The bigger size of NS as compared to the smectic layer separation causes the warping in the smectic layer. Semiconducting nature of NS also affects the conductivity of the pure FLC.

1. Introduction

The scope of nanotechnology, in the present age, is not only limited within the field of material science but also extended to all the fields of research and application. The fields like electronics, condense matter, and medical sciences are benefited from the application point of view when used with nanoscience [1–3]. The use of nanoscience in fields of liquid crystal has created some interesting and useful properties [4].

Ferroelectric liquid crystals (FLCs) have salient features over the trivial liquid crystals (LCs) because of their tilted smectic phase and the chirality of the molecules [5]. They have proved their applicability of showing faster response time and the instruments based on less threshold voltage [6]. In addition to these properties, they have also shown their potential for the field effect transistors (FETs), spatial light modulators (SLMs), switchable devices, and nonvolatile memory effects [7, 8]. The prospective of tuning the properties of liquid crystals due to the addition of nanomaterial is currently a hot topic in liquid crystal research [9–11]. The composite system of the pure FLC and nanomaterial has already shown its utility in the FLC-based devices with greater efficiency [12].

In the present paper, we report a comprehensive study of the dielectric and electro-optical (E-O) properties of a ferroelectric liquid crystal highly doped with $ZnO_{1-x}S_x$ nanospheres (NS). The present work has a motive to analyze the effect of high concentration of the nanomaterial on the FLC matrix and also on the E-O and dielectric parameters. The $ZnO_{1-x}S_x$ NS were added in 5% wt/wt concentration to the pure FLC 16/100. The results show that the doping of NS alters the physical properties of the pure FLC. The investigated results are discussed and explained on the basis of the interactions taking place between the NS and FLC molecules in the composite geometry, effect of high doping of NS on the pure FLC, and molecular dynamics of NS and FLC molecules with their dipolar contributions.

2. Experimental Details

A commercially available ferroelectric liquid crystal (FLC) 16/100, purchased from Clariant Chemicals Co. Ltd., Germany, was used as host material in the present study.

The phase sequence of the FLC material is Cr, SmC*, SmA, N*, and Iso at −20°C, 72°C, 82°C, and 90°–94°C. For the pure FLC 16/100, the standard values (as provided by the manufacturer) of spontaneous polarization (P_s), cone angle (2θ), and rotational viscosity (γ_G) at 25°C were −10.5 nC/cm^2, 54.30°, and 60 m Pa.s, respectively.

The $ZnO_{1-x}S_x$ nanospheres (NS) were added to the pure FLC as a guest entity. A typical coprecipitation method was used to synthesize the present NS (nanocrystals of spherical shape) taking CH_3OH as solvent. The prepared NS were characterized by X-ray diffraction (XRD) and transmission electron microscopy (TEM). The diameter of the nanospheres was found to be ~10–15 nm. The detailed information about the synthesis of the nanosphere (spherical shape nanoparticle) and the effect of small concentration of the NS on FLC parameters has already been published by Singh et al. [13].

Highly conducting (~ 20 Ω/□) indium tin oxide (ITO) coated glass plates were used to make sample cells. The desired electrode pattern on the ITO substrates was achieved using a photolithographic technique. The active electrode area was 7 mm × 7 mm. The uniform thickness (6 μm in our case) of both the sample cells was maintained by means of Mylar spacer. The planar alignment was obtained by coating polymer (Nylon 6/6) on ITO glass plate and unidirectional rubbing. The empty sample cells were calibrated using analytical reagent (AR) grade carbon tetrachloride (CCl_4) and benzene (C_6H_6).

The nanosphere-ferroelectric liquid crystal (NS-FLC) composite system was prepared by the mixing of NS in the 5% wt/wt ratio with pure FLC 16/100. To prepare the composite system, an appropriate amount (in the weight ratio, i.e., 5.0%) of nanospheres was mixed into the pure FLC and then homogenized with an ultrasonic mixer at 90°C for one hour, and uniform dispersion of nanospheres was ensured but the high concentration of NS aggregates in the pure FLC matrix which was clearly observed in the polarizing optical microscope (POM) images.

The pure FLC and the NS-doped FLC were filled in the sample cells at a temperature higher than the isotropic temperature by means of capillary action and then cooled gradually up to room temperature with the application of a small a.c. electric field. The alignment of the samples was checked by the polarizing microscope under the crossed polarizer-analyzer arrangement.

The dielectric spectroscopy of the samples was performed by a computer-controlled impedance/gain analyzer (Solartron SL1260) attached with a temperature controller for the frequency interval 100 Hz–32 MHz. The dielectric measurements were carried out as a function of temperature by placing the sample on a computer-controlled hot plate instec (HCS 302). The temperature stability was better than ±0.1°C. The low- and high-frequency corrections were also made to the experimental data.

The FTIR spectra of the pure and the NS-doped FLC was recorded by the Fourier transform infrared spectrophotometer (IR Affinity-1, SHIMADZU) between 1500 to 3000 cm^{-1}. The photoluminescence (PL) spectra of pure and NS-doped FLC were recorded using Perkin Elmer LS 55 luminescence spectrophotometer. During the PL measurement, all the measuring parameters like slit width (4 nm in our case), excitation step, and so forth, were same for the entire samples. The two excitation wavelengths, that is, 290 and 315 nm, were used to record the PL spectra of the pure and the NS-doped FLC in the present investigation.

The spontaneous polarization (P_s) measurement was performed using a triangular wave method at a voltage of 20 $V_{P\text{-}P}$ and 10 Hz frequency. P_s was determined by using the following relation [14]:

$$P_s = \frac{1}{2A}\int i(t)\,dt, \tag{1}$$

where $\int i(t)dt$ is the area under the current bump and A is the active area of the sample in sample holder. For the measurement of response time (τ_{res}), a square wave signal of 10 Hz and 20 $V_{P\text{-}P}$ was used. The rotational viscosity (γ_G) of the Goldstone mode in SmC* phase was calculated by the relation

$$\gamma_G = P_s \times \tau_{res} \times E = P_s \times \frac{t_{10} - t_{90}}{1.8} \times E, \tag{2}$$

where E is the applied switching field and t_{10} and t_{90} are the corresponding times for 10% and 90% of the maximum level of response time while other symbols have their usual meaning [15].

The dielectric relaxation phenomena of the pure and the NS-doped FLC were analyzed using the Cole-Cole relation [16]:

$$\varepsilon^* = \varepsilon'(\infty) + \frac{\delta\varepsilon}{1 + (i\omega\tau)^{1-\alpha}}, \tag{3a}$$

where, $\delta\varepsilon$ is the relaxation strength and $\varepsilon'(\infty)$ is the high-frequency limit of the dielectric permittivity data, $\omega = 2\pi f$, where f is the frequency, τ is the relaxation time, and α is the distribution parameter. The experimental data suffers low- and high-frequency deviations in dielectric data and exceedingly require correction for low- and high-frequency values. On separating the real and imaginary parts of (3a), one may get

$$\varepsilon' = \varepsilon'(dc)\, f^{-n} + \varepsilon'(\infty) + \frac{\delta\varepsilon\left[1 + (2\pi f\tau)^{(1-\alpha)}\sin(\alpha\pi/2)\right]}{1 + (2\pi f\tau)^{2(1-\alpha)} + 2(2\pi f\tau)^{(1-\alpha)}\sin(\alpha\pi/2)}, \tag{3b}$$

$$\varepsilon'' = \frac{\sigma(dc)}{\varepsilon_0 2\pi f^k} + \frac{\delta\varepsilon(2\pi f\tau)^{(1-\alpha)}\cos(\alpha\pi/2)}{1 + (2\pi f\tau)^{2(1-\alpha)} + 2(2\pi f\tau)^{(1-\alpha)}\sin(\alpha\pi/2)} + Af^m. \tag{3c}$$

Here, $\sigma(dc)$ is the dc ionic conductance, ε_o is the free space permittivity, and f is the frequency while n, m, and k are the fitting parameters. The terms $\varepsilon'(dc)f^{-n}$ and $\sigma(dc)/\varepsilon_o 2\pi f^k$

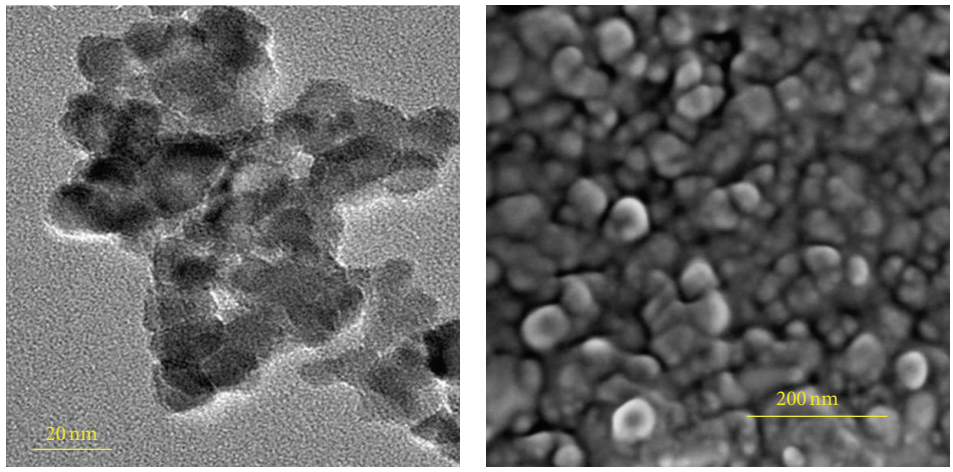

(a) (b)

Figure 1: (a) The scanning electron microscopic (SEM) image of the $ZnO_{1-x}S_x$ nanosphere (NS) which represents a small agglomeration of the NS. (b) SEM image of the aggregation of NS.

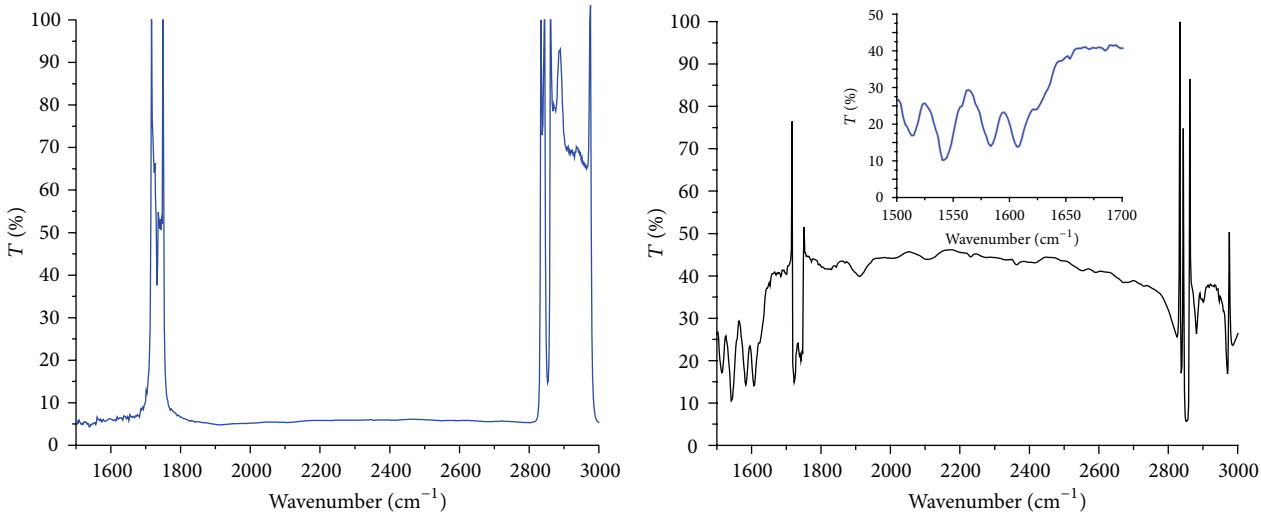

(a) (b)

Figure 2: FTIR spectra of the (a) pure FLC and (b) NS-doped FLC material. The inset of Figure 2(b) shows the enlarged FTIR spectra of the NS-doped FLC material between the interval of 1500–1700 cm^{-1}.

are added in (3b) and (3c) for correcting the low-frequency effect due to the electrode polarization capacitance and ionic conductance. The Af^m term is added in (3c) for correcting the high-frequency effect due to the ITO resistance and lead inductance [9]. The other abbreviations are same as given for (3a). The experimental data have been fitted in these equations and corrected for low- and high-frequency values [13].

3. Results and Discussions

Figures 1(a) and 1(b) represent the SEM image of the $ZnO_{1-x}S_x$ (NS) and aggregation of the NS, respectively. A small agglomeration has been observed in the SEM image of the NS which is the basic problem of most of the nanomaterial. Due to the agglomeration property of NS, it aggregates in the FLC matrix as dispersed in high concentration. The aggregation and topological defects are the main factors which alter the physical properties of the pure FLC material.

Fourier transform infrared (FTIR) spectroscopy is a powerful modern technique for the characterization of samples. This technique provides the information about the concentration of the impurities, their bonding with the host material, and different types of vibrations occurring in the samples. The FTIR analysis, for the wave number intervals of 1500–3000 cm^{-1}, has been performed for the pure and the NS-doped FLC material in Figures 2(a) and 2(b), respectively. The change in FTIR spectra for the NS-doped FLC system is mainly due to the aggregation of the NS in FLC matrix. As, NS behaves like the ionic additive to the FLC matrix, the large concentration of the NS (or aggregation of NS) reflects in the FTIR spectra in the form of impurity. The inset of Figure 2(b)

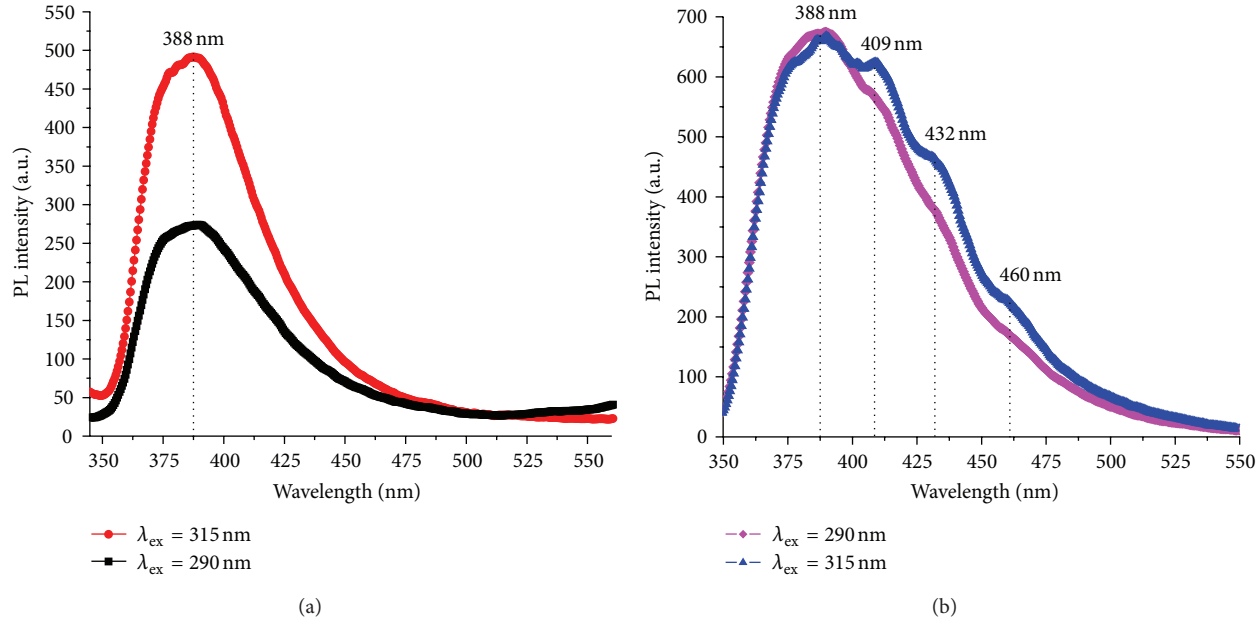

FIGURE 3: The photoluminescence (PL) spectra of the (a) pure FLC and the (b) NS-doped FLC at two different excitation wavelengths, that is, 290 nm and 315 nm.

shows the enlarged image of FTIR spectra from 1500 to 1700 cm^{-1}. The transmission peaks in this region show the vibrations corresponding to impurity ions, that is, NS. The change in percentage Transmission is due to the topological defects and scattering of light from the aggregation of NS. Therefore, the change in FTIR spectra clearly indicates the presence of a guest entity in a large concentration in the FLC matrix.

The PL spectra of the pure and the NS-doped FLC using two different excitation wavelengths have been shown in Figure 3. The PL spectra of the pure FLC show a broad emission peak centred at 388 nm corresponding to violet emission. The PL measurement was performed on two different excitation wavelengths, that is, 290 nm and 315 nm. The change in the excitation wavelength only alters the intensity of emission peak, but it does not cause any shifting in the emission peak. Due to the addition of NS, the PL of the pure FLC materials has been enhanced. This enhancement in the PL spectra of the pure FLC materials is attributed to the coupling of localized surface plasmon resonance from NS with FLC molecules [17]. In addition to this, some other feeble PL emission peaks centred at 409, 432, and 460 nm have also been observed. These emission peaks lie in the spectral region due to the self-activated PL centres. These centres have often been attributed to the crystal vacancies. Thus, feeble PL emission peaks centred at 409, 432, and 460 nm arise from the crystal line incorporation of trace amount of Zn^{2+} in the crystal lattice creating the oxygen and sulphur deficiency [18]. The nonsmoothening of the PL spectra also suggests the size distribution of the NS in FLC matrix. The change in excitation wavelength does not produce any change in the magnitude of the PL emission peak of the NS-doped FLC system. This shows that the aggregation of the NS in the pure FLC matrix due to large amount of NS dominate over the intras FLC interactions.

With the help of triangular wave electrical response curve (also known as polarization reversal current method), the spontaneous polarization of the pure and the NS-doped FLC has been calculated. The behaviour of spontaneous polarization (P_s) with the change in temperature is shown in Figure 4(a). The value of P_s decreases with increasing temperature for both the pure and the doped FLC, but the P_s value for the NS doped FLC system is higher than that of the pure FLC. When a high concentration of the NS is dispersed in the FLC material, it causes an aggregation of the NS. The NS behaves like an ionic additive in the FLC system. At the place of aggregation, these ionic charges accumulate and form a local internal electric field. This local internal electric field increases the separation between polarization charges on the LC molecules which results in the increased dipole moment of the doped system. The increased dipole moments result the increased spontaneous polarization of the NS-doped FLC system [19].

The response time (τ_{res}) of the pure and the doped FLC system is plotted against the temperature scale in Figure 4(b). The response time of the pure and the doped system decreases with increasing temperature. The response for the doped system is slower as compared to the pure FLC due to the presence of high concentration of NS. The presence of high quantity of NS creates additional constraints in the molecular motion of the FLC molecules under the influence of applied field. These constraints reduce the energy of the doped FLC system; therefore, FLC molecules do not respond quickly with the applied field as compared to the pure FLC molecules which results in a slower response for the NS-FLC system. No noticeable shift in the SmC^*-SmA phase

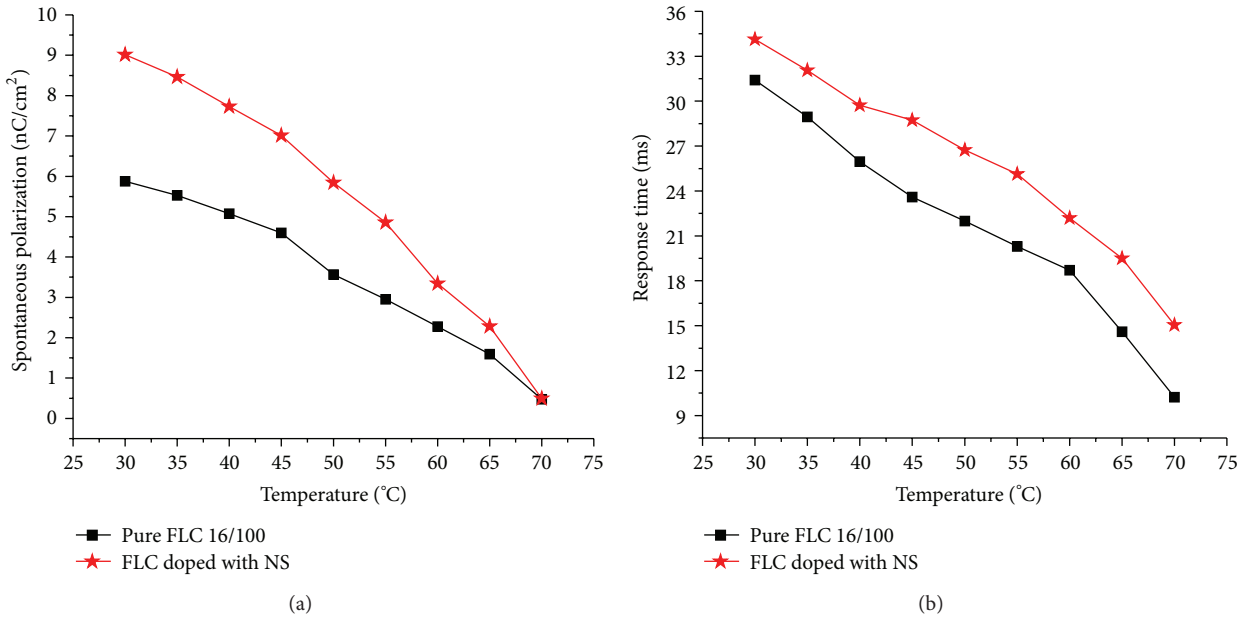

FIGURE 4: The variation of (a) spontaneous polarization and (b) response time on the temperature scale for the pure and the NS-doped FLC samples.

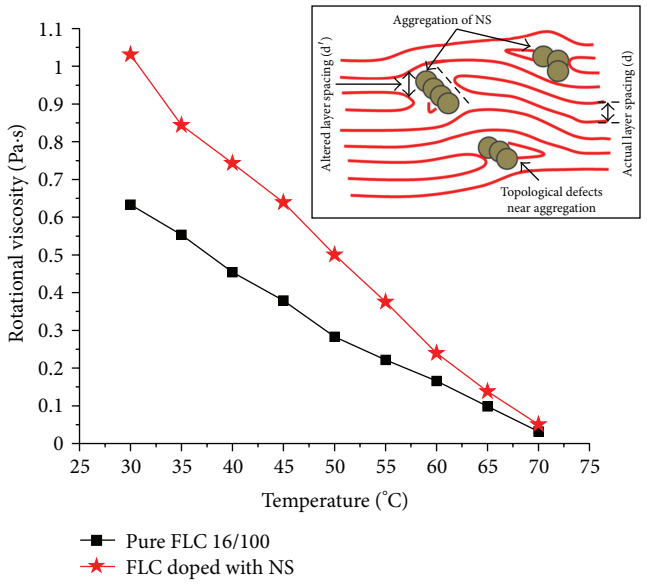

FIGURE 5: The change in rotational viscosity with the variation of temperature for the pure and the NS-doped FLC whereas the inset of figure shows the paradigm of the warping of the smectic layers due to the presence of aggregation of NS.

transition temperature has been observed for the NS-FLC system.

The rotational viscosity with the variation of temperature is shown in Figure 5. Almost linear decrement in the value of rotational viscosity on increasing the temperature has been observed for both the pure and the doped systems. But the value of rotational viscosity for the NS-doped FLC system is greater than that of the pure FLC system. As rotational viscosity ($\gamma = P_s \cdot \tau_{\text{res}} \cdot E$) is the product of spontaneous polarization, response time, and effective electric field applied on the sample cell, therefore due to increase in the spontaneous polarization and response time, the rotational viscosity also increases as compared to the pure FLC material. As discussed previously, the NS aggregates in the FLC matrix and forms a local internal electric field near the aggregation. This field influences the smectic layer ordering which alters the smectic layer spacing as shown in the inset of Figure 5. This combined effect of disordering in smectic layers and aggregation produces the topological defects in FLC matrix. These two factors affect the rotational motion of FLC molecules which results in the enhanced rotational viscosity of the doped FLC system. The alteration in the smectic layer separation due to spherical gold nanoparticle has already been reported by Pratibha et al. [20].

In the molecular motion of the composite system, four types of interactions take place, namely,

(i) FLC molecule-molecule interaction;

(ii) FLC molecule-NS interaction;

(iii) NS-NS interaction;

(iv) FLC molecule-alignment layer interaction.

In the presence of any guest entity (nanoparticles, CNTs, dyes, polymers, etc.), the interaction of FLC molecules with that of the guest material (NS in our case) takes place. The probability of weak or strong NS-NS interaction depends upon the concentration of NS in the composite system. In the present work, 5% wt/wt concentration of NS causes strong NS-NS interactions in the composite system. This strong NS-NS interaction causes the aggregation of NS in FLC matrix. One should notice that the size of the nanomaterial also

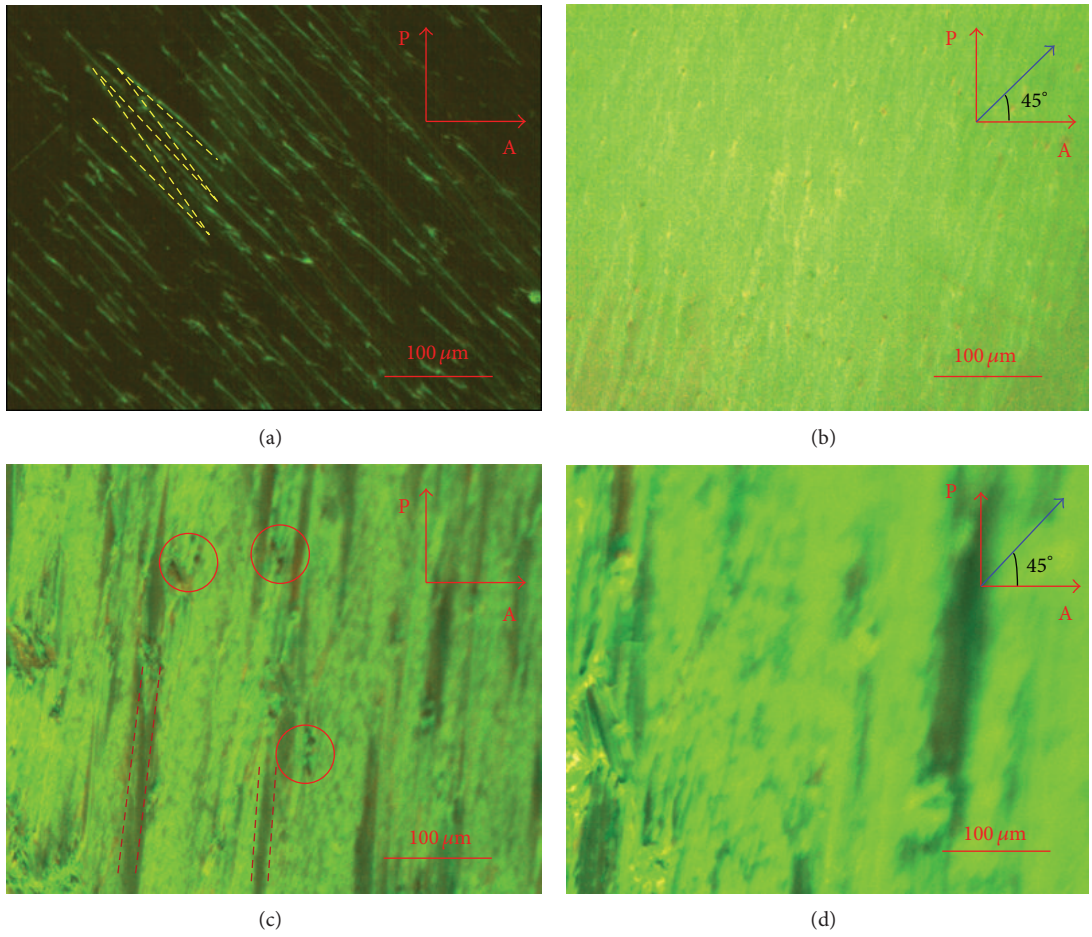

FIGURE 6: Polarizing optical microscopic (POM) texture in dark state (a) pure FLC, (c) NS-doped FLC, bright state (b) pure FLC, and (d) NS-doped FLC. The dark state was achieved under the crossed polarizer-analyzer condition whereas the bright state was achieved by rotating the sample cell by 45° from the initial condition. The aggregation of NS has been shown in the circle and topological defects are shown between two dotted parallel lines. Chevron or zig-zag defects are shown in Figure 6(a) in V-shaped dotted lines.

plays a crucial role in determining the properties of the composite systems [21]. The bigger size of NS and strong NS-NS interaction are mainly responsible for the modifications in the properties of the pure FLC. From the application point of view, FLC-NS interaction in the composite is accountable depending on the nature, characteristics, size, shape, and quantity of NS.

Mainly, three types of events exist in the NS-FLC composite system; that is, the presence of NS wraps the smectic layers around it, NS produces hindrance in the motion of the FLC molecule, and NS strongly interacts with the FLC molecules. The presence of NS warps the smectic layers and alters the spacing between them. These warped smectic layers radically alter the neighbouring smectic layers. In the cone motion of the FLC molecules, the factor $d\varphi/dt$ in viscous torque ($-\Gamma_z = \gamma(d\varphi/dt)$, where Γ_z is the z component of viscous torque and φ is the phase angle) is redistributed because of the warping of the smectic layers. This results in a higher rotational viscosity for the NS-doped FLC system.

The polarizing optical microscopic (POM) images in dark and bright states have been shown in Figure 6. Figures 6(a) and 6(b) represent the POM images of the pure FLC in dark and bright states, respectively, whereas Figures 6(c) and 6(d) represent the NS-doped FLC in the dark and bright states. The dark state POM image corresponds to undercrossed polarizer-analyzer condition whereas the bright state was achieved by rotating the sample cell by 45° from the initial condition. The high concentration of NS causes aggregation and defects in the FLC medium which is clear from Figure 6(c). Due to this aggregation of NS, the molecular ordering of the FLC molecules also impairs. The increase in the relaxation strength of the NS-doped FLC is compatible with the present result. The study of the relaxation strength will be discussed later in the paper. The high doping of the NS in the pure FLC also reduces the anchoring of the FLC sample which is also verified by the optical textures. The occurrence of the intense chevron geometry can be seen in the case of the pure FLC (Figures 6(a) and 6(b)) whereas in the doped FLC system, the chevron geometry was not well observed. The presence of high concentration of the NS causes other topological defects in the FLC matrix causing the scattering of transmitted light through NS which lowers

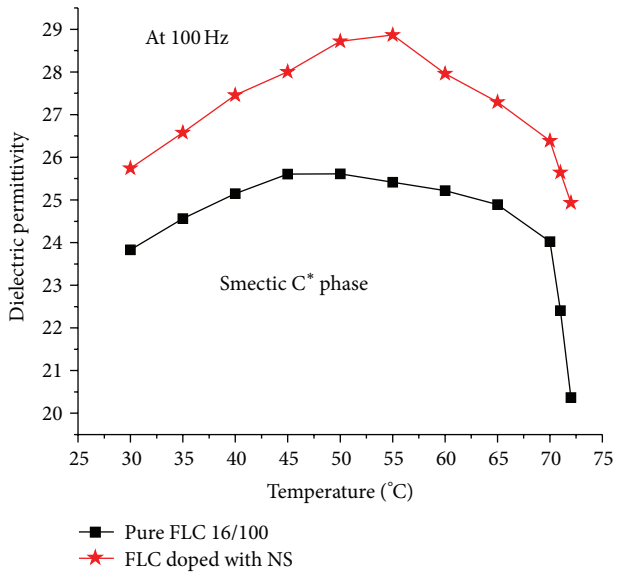

FIGURE 7: Temperature dependence of the dielectric permittivity at 100 Hz for the pure and the NS-doped FLC.

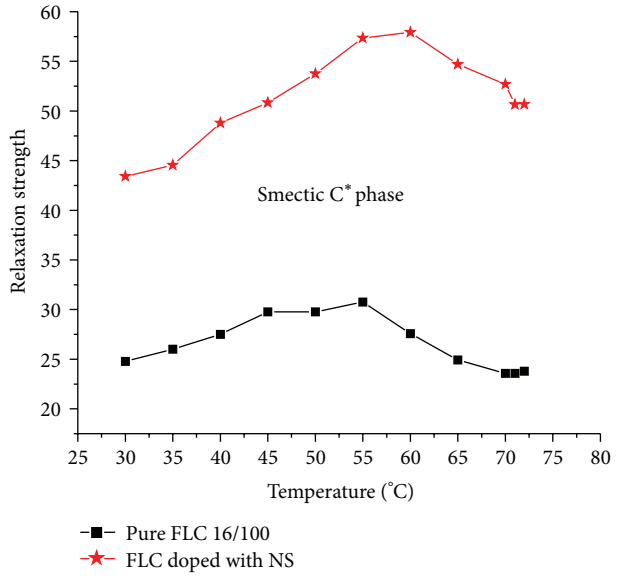

FIGURE 8: The variation of the relaxation strength with change in temperature for the pure and the NS-doped FLC.

the contrast of the NS-doped FLC system. From application point of view, the controlled addition of nanomaterial in liquid crystal enhances the contrast of the LC material; therefore, the determination of the suitable concentration of any nanomaterial in host LC is vital factor.

The change in response time can also be understood by this observation. For weak anchoring, the relation can be given as [22]

$$\tau_{\text{Res}} = \frac{4\eta d}{W\pi^2}, \tag{4}$$

where d is the cell thickness and W is the anchoring energy coefficient. The lower anchoring energy coefficient of the NS-doped FLC results in a higher response time.

The temperature dependence of the dielectric permittivity at 100 Hz for both the pure and the NS-doped FLC is depicted in Figure 7. The dielectric permittivity of the pure FLC increases slightly with increase in the temperature. The maximum value of dielectric permittivity for the pure FLC has been noticed at 45°C. Further increment in temperature causes a small decrease in the dielectric permittivity. A sharp decrement in the value of dielectric permittivity has been observed at the vicinity of SmC*-SmA phase transition temperature. This sharp decrease in the dielectric permittivity is due to the change in geometry at the SmC*-SmA phase transition temperature. The dielectric permittivity measurement for the NS-doped FLC shows an increased value of this parameter as compared to the pure FLC. This increase in the value of dielectric permittivity is due to the increased polarization (i.e., net dipole moment) of the NS-FLC system [23]. The variation of dielectric permittivity on temperature scale for the NS-doped FLC is not similar to that of the pure FLC. For the NS doped FLC system, the value of dielectric permittivity increases almost linearly with increase in the temperature for the temperature interval of 30°C–55°C. Beyond this temperature interval, the dielectric permittivity shows a reducing trend on the temperature scale due to the change in geometry of the LC phase.

The relaxation strength ($\Delta\varepsilon$) is plotted against the temperature in Figure 8. The relaxation strength for both the pure and the NS-doped FLC increases with increase in the temperature. The relaxation strength shows its maximum value near the temperature 55°C, and further increment in temperature causes a decrease in the value of $\Delta\varepsilon$ because FLC sample approaches from SmC* to SmA phase. The relaxation strength for the doped FLC system is greater than that of the pure FLC. This greater value of $\Delta\varepsilon$ for the doped system can be explained by the following relation [24]:

$$\Delta\varepsilon = \frac{1}{2K\varepsilon_0} \cdot \frac{P_s^2}{q^2\theta^2}, \tag{5}$$

where $\Delta\varepsilon$ is the relaxation strength, P_s the spontaneous polarization, θ the tilt angle, q the wave vector of helix, and K is the elastic constant. The quantity P_s/θ is a constant in the first approximation and the variation of K with temperature is also very small; therefore, the variation of relaxation strength mainly depends upon the wave vector of helix (q). The wave vector of helix ($q = 2\pi/p$, where p is pitch) is decreased; thus, p increases due to aggregation of NS and defects formation in the FLC matrix.

A nonlinear increase in relaxation frequency (f_R) has been shown in Figure 9. In the whole SmC* phase, relaxation frequency increases nonlinearly with increasing temperature and attains its maximum value at SmC*-SmA phase transition temperature. Further increment in the temperature causes a sharp decrease in the relaxation frequency value due to change in phase geometry and the removal of helical structure of the FLC molecules. The value of relaxation frequency for the doped FLC system is less as compared to

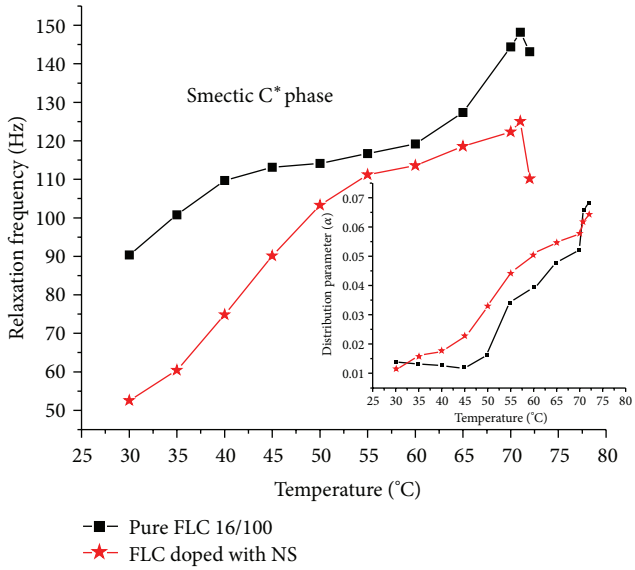

Figure 9: The variation of the relaxation frequency with change in temperature for the pure and the NS-doped FLC while the inset of figure shows the variation of the distribution parameter with change in temperature.

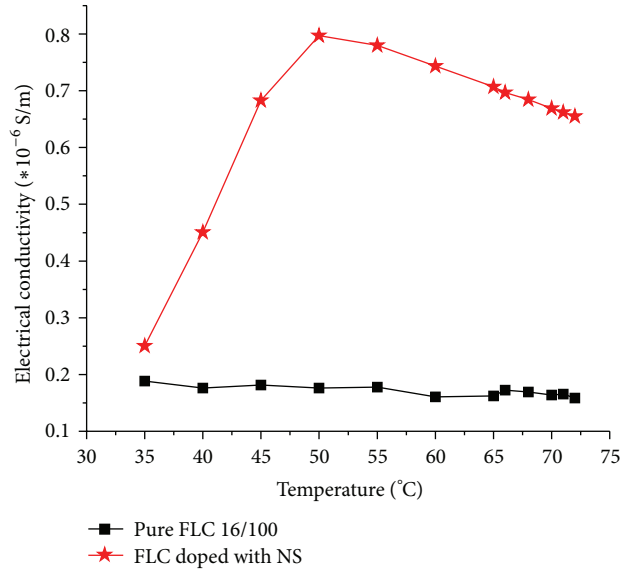

Figure 10: The change in the electrical conductivity with the variation of temperature for the pure and the NS-doped FLC.

the pure FLC system. This behaviour of f_R can be explained by the relation [25]

$$f_R = \frac{Kq^2}{2\pi\gamma}, \tag{6}$$

where γ is the rotational viscosity and other symbols have their usual meaning.

The above relation shows that relaxation frequency is inversely proportional to the rotational viscosity. As the rotational viscosity has greater value for the doped system, a reduced value of the relaxation frequency is found for it. In addition to this, the relaxation frequency also depends upon the wave vector of helix. It is assumed that the wave vector of helix has also decreased due to the presence of NS which results in the decrease in relaxation frequency. The reduction in the relaxation frequency has also verified by the distribution parameter (α) shown in the inset of Figure 9. The value of α is higher for the NS-doped FLC sample; therefore, the relaxation frequency of the NS-doped FLC get reduced. The distribution parameter of the pure FLC is almost constant for the first four consecutive observations on temperature scale (i.e. 30°C to 45°C). Beyond these observations, distribution parameter increases with increase in the temperature. For the NS doped FLC system, distribution parameter also increases with increase in the temperature. In both cases, the small value of distribution parameter (0.01–0.07) indicates that Goldstone mode predominates over the soft mode in the SmC* phase [26], and the doped FLC system completely follows the Cole-Cole-type relaxation process.

Figure 10 represents the change in electrical conductivity [27] with the variation of temperature at 133 Hz for both the pure and the NS-doped FLC. For the pure FLC system, the electrical conductivity is almost temperature independent whereas it strongly depends on temperature for the NS-doped FLC system. Electrical conductivity sharply increases with increase in the temperature and shows its maximum value at 50°C. Further increment in the temperature causes a reduction in the electrical conductivity. As NS behaves like the ionic additives to the FLC materials, it increases the electrical conductivity in the doped FLC system. In the temperature range of 35°C–50°C, the conductivity is mainly driven by the semiconducting nature of the NS, and conductivity increases with increase in the temperature. Beyond 50°C, the FLC molecules get sufficient energy and move with more kinetic energy which increases the number of collisions of FLC molecules with NS. Thus, the resistive forces increase in the NS-FLC system which results in the decrement in the conductivity.

4. Conclusions

The salient features of the present investigation can be concluded as follows: the addition of nanospheres (NS) in the pure FLC material changes the dielectric and E-O parameters of the pure FLC. The bigger size of NS occupies greater volume as compared to the FLC molecule; therefore, they produce hindrance in the motion of the FLC molecules and wrap the smectic layer. The high quantity of NS produces strong NS-NS interaction (which causes the aggregation of NS in the FLC matrix) which dominates other interactions taking place in the composite system. The presence of high concentration of NS was confirmed by the FTIR analysis. The change in FTIR spectra clearly indicates the presence of a guest entity. The change in percentage transmission in the NS-doped FLC system is due to the topological defects and scattering of the light from the aggregation of NS in FLC matrix. The enhanced PL in case of the NS-doped FLC has been attributed to the surface Plasmon resonance between the

NS and FLC molecules. Some other secondary PL emission peak has also been noticed due to the result of the oxygen and sulphur vacancies in the crystal structure. The aggregation of NS supports the FLC molecular dipole moment which increases the net ferroelectricity (or net dipole moment) in the composite. The increased ferroelectricity increases the value of spontaneous polarization and dielectric permittivity. The variation of relaxation strength and relaxation frequency depends upon the wave vector of helix and rotational viscosity. The distribution parameter strongly recommends for the existence of Cole-Cole relaxation phenomena in the composite system. The topological defects, produced by NS, create a slower response for the composite system, but its order is still important in case of constant rate video processing. High dopant concentration of the NS (i.e., 5%) in FLC plays a role as ionic additive which results in a higher conductivity for the NS-doped FLC system. The better electrical response in the NS doped FLC system indicates its applicability in electronic device fabrication. The intense chevron geometry in case of the pure FLC has not been observed in the NS-doped FLC system, but the high concentration of NS produces the topological defects in the composite system.

Acknowledgments

The authors are thankful to the Department of Science and Technology, Government of India, for the financial assistance for present work in the form of project. The authors (Swadesh Kumar Gupta and Dharmendra Pratap Singh) are thankful to CSIR for SRF Grant. Authors are also very thankful to Professor A. C. Pandey, Nano Application Centre, University of Allahabad, for providing the nanospheres for present study.

References

[1] L. J. Yu and M. M. Labes, "Fluorescent liquid-crystal display utilizing an electric-field-induced cholesteric-nematic transition," *Applied Physics Letters*, vol. 31, no. 11, pp. 719–720, 1977.

[2] R. C. Y. King and F. Roussel, "Transparent carbon nanotube-based driving electrodes for liquid crystal dispersion display devices," *Applied Physics A*, vol. 86, no. 2, pp. 159–163, 2007.

[3] L. Calucci, G. Ciofani, D. de Marchi et al., "Boron nitride nanotubes as T_2-weighted MRI contrast agents," *Journal of Physical Chemistry Letters*, vol. 1, no. 17, pp. 2561–2565, 2010.

[4] D. P. Singh, S. K. Gupta, A. Srivastava, and R. Manohar, "The phenomenon of induced photoluminescence in ferroelectric mesophase," *Journal of Luminescence*, vol. 139, pp. 60–63, 2013.

[5] R. B. Meyer, L. Liebert, L. Strzelecki, and P. Keller, "Ferroelectric liquid crystals," *Journal de Physique Lettres*, vol. 36, no. 3, pp. 69–71, 1975.

[6] T. Joshi, A. Kumar, J. Prakash, and A. M. Biradar, "Low power operation of ferroelectric liquid crystal system dispersed with zinc oxide nanoparticles," *Applied Physics Letters*, vol. 96, no. 25, Article ID 253109, 3 pages, 2010.

[7] R. Martel, V. Derycke, C. Lavoie et al., "Ambipolar electrical transport in semiconducting single-wall carbon nanotubes," *Physical Review Letters*, vol. 87, no. 25, Article ID 256805, 4 pages, 2001.

[8] J. Prakash, A. Choudhary, A. Kumar, D. S. Mehta, and A. M. Biradar, "Nonvolatile memory effect based on gold nanoparticles doped ferroelectric liquid crystal," *Applied Physics Letters*, vol. 93, no. 11, Article ID 112904, 3 pages, 2008.

[9] D. P. Singh, S. K. Gupta, K. K. Pandey, S. P. Yadav, M. C. Varia, and R. Manohar, "Ferroelectric liquid crystal matrix dispersed with Cu doped ZnO nanoparticles," *Journal of Non-Crystalline Solids*, vol. 363, pp. 178–186, 2013.

[10] V. N. Vijayakumar and M. L. N. M. Mohan, "Enhancement of the display parameters of 4′-pentyl-4-cyanobiphenyl due to the dispersion of functionalised gold nano particles," *Journal of Dispersion Science and Technology*, vol. 33, no. 1, pp. 111–116, 2012.

[11] A. Kumar, G. Singh, T. Joshi, G. K. Rao, A. K. Singh, and A. M. Biradar, "Tailoring of electro-optical properties of ferroelectric liquid crystals by doping Pd nanoparticles," *Applied Physics Letters*, vol. 100, no. 5, Article ID 054102, 4 pages, 2012.

[12] A. K. Srivastava, E. P. Pozhidaev, V. G. Chigrinov, and R. Manohar, "Single walled carbon nano-tube, ferroelectric liquid crystal composites: excellent diffractive tool," *Applied Physics Letters*, vol. 99, no. 20, Article ID 201106, 3 pages, 2011.

[13] D. P. Singh, S. P. Yadav, P. K. Tripathi et al., "Concentration dependent physical parameters of ferroelectric liquid crystal and ZnOS nano material composite system," *Soft Materials*, vol. 11, no. 3, pp. 305–314, 2013.

[14] R. Manohar, A. K. Srivastava, P. K. Tripathi, and D. P. Singh, "Dielectric and electro-optical study of ZnO nano rods doped ferroelectric liquid crystals," *Journal of Materials Science*, vol. 46, no. 18, pp. 5969–5976, 2011.

[15] K. Skarp and S. T. Lagerwall, "Rotational viscosities in ferroelectric smectic liquid crystals," *Ferroelectrics*, vol. 84, no. 1, pp. 119–142, 1988.

[16] K. S. Cole and R. H. Cole, "Dispersion and absorption in dielectrics I. Alternating current characteristics," *The Journal of Chemical Physics*, vol. 9, no. 4, pp. 341–351, 1941.

[17] A. Kumar, J. Prakash, D. S. Mehta, A. M. Biradar, and W. Haase, "Enhanced photoluminescence in gold nanoparticles doped ferroelectric liquid crystals," *Applied Physics Letters*, vol. 95, no. 2, Article ID 023117, 3 pages, 2009.

[18] A. Kumar, J. Prakash, A. D. Deshmukh, D. Haranath, P. Silotia, and A. M. Biradar, "Enhancing the photoluminescence of ferroelectric liquid crystal by doping with ZnS quantum dots," *Applied Physics Letters*, vol. 100, no. 13, Article ID 134101, 4 pages, 2012.

[19] P. Malik, A. Chaudhary, R. Mehra, and K. K. Raina, "Electrooptic and dielectric studies in cadmium sulphide nanorods/ferroelectric liquid crystal mixtures," *Advances in Condensed Matter Physics*, vol. 2012, Article ID 853160, 8 pages, 2012.

[20] R. Pratibha, W. Park, and I. I. Smalyukh, "Colloidal gold nanosphere dispersions in smectic liquid crystals and thin nanoparticle-decorated smectic films," *Journal of Applied Physics*, vol. 107, no. 6, Article ID 063511, 5 pages, 2010.

[21] F. V. Podgornov, A. V. Ryzhkova, and W. Haase, "Influence of gold nanorods size on electro-optical and dielectric properties of ferroelectric liquid crystals," *Applied Physics Letters*, vol. 97, no. 21, Article ID 212903, 3 pages, 2010.

[22] X. Nie, R. Lu, H. Xianyu, T. X. Wu, and S. Wu, "Anchoring energy and cell gap effects on liquid crystal response time," *Journal of Applied Physics*, vol. 101, no. 10, Article ID 103110, 5 pages, 2007.

[23] S. K. Gupta, D. P. Singh, and R. Manohar, "SWCNT doped ferroelectric liquid crystal: the electro-optical properties with enhanced dipolar contribution," *Current Applied Physics*, vol. 13, no. 4, pp. 684–687, 2013.

[24] T. P. Majumder, M. Mitra, and S. K. Roy, "Dielectric relaxation and rotational viscosity of a ferroelectric liquid crystal mixture," *Physical Review E*, vol. 50, no. 6, pp. 4796–4800, 1994.

[25] H. S. Kitzerow and C. Bahr, *Chirality in Liquid Crystals*, Springer, Berlin, Germany, 2001.

[26] Y. P. Panarin, Y. P. Kalmykov, S. T. M. Lughadha, H. Xu, and J. K. Vij, "Dielectric response of surface stabilized ferroelectric liquid crystal cells," *Physical Review E*, vol. 50, no. 6, pp. 4763–4772, 1994.

[27] F. Kremer and A. Schonhals, *Broadband Dielectric Spectroscopy*, Springer, Berlin, Germany, 2003.